**Did Late Miocene (Messinian) gypsum precipitate from evaporated marine brines? Insights from the Piedmont Basin (Italy)**

Publisher: GSA
Journal: GEOL: Geology
Article ID: G34986

# Did the Late Miocene (Messinian) gypsum precipitate from evaporated marine brines? Insights from the Piedmont Basin (Italy)

**Marcello Natalicchio[1]*, Francesco Dela Pierre[1], Stefano Lugli[2], Tim K. Lowenstein[3], Sarah J. Feiner[3], Simona Ferrando[1], Vinicio Manzi[4], Marco Roveri[4], and Pierangelo Clari[1]**

[1]*Dipartimento di Scienze della Terra, Università di Torino, 10125 Torino, Italy*

[2]*Dipartimento di Scienze Chimiche e Geologiche, Università di Modena e Reggio Emilia, 41100 Modena, Italy*

[3]*Department of Geological Sciences & Environmental Studies, State University of New York, Binghamton, 13902 New York, USA*

[4]*Dipartimento di Fisica e Scienze della Terra, Università di Parma, 43100 Parma, Italy*

*E-mail: marcello.natalicchio@unito.it.

**ABSTRACT**

During the first stage of the Late Miocene Messinian salinity crisis (5.97 - 5.60 Ma) deposition of sulfates (Primary Lower Gypsum) occurred in shallow silled peripheral sub-basins of the Mediterranean experiencing restricted water exchange with the Atlantic Ocean. Fluid inclusions in Messinian selenite crystals from the Piedmont Basin (NW Italy) have surprisingly low salinities (average of 1.6 weight % NaCl equivalent), suggesting parent waters depleted in $Na^+$ and $Cl^-$ compared to modern seawater. Modern gypsum from a Mediterranean saltwork, in contrast, contains fluid inclusions with elevated salinities that match the normal evaporation trend expected for seawater. The salinity data indicate that the Messinian sulfate deposits from the Piedmont Basin formed from hybrid parent waters: seawater mixed with $Ca^{2+}$ and $SO_4^{2-}$ enriched freshwaters that dissolved coeval marginal

marine gypsum. Such mixed parent waters and complex recycling processes should be taken into account when explaining the genesis of other Messinian gypsum deposits across the Mediterranean Basin.

## INTRODUCTION

Since the 1970s, numerous studies have reconstructed the depositional paleoenvironments of Late Miocene sulfates and the paleohydrology of the Mediterranean during the Messinian salinity crisis (CIESM, 2008). However, estimates of the composition and salinity of brines from which large volumes of sulfates formed are still scarce and have been mostly obtained by isotope geochemistry (e.g., Pierre and Fontes, 1978; Longinelli, 1979). Chemical analyses of fluid inclusions in saline minerals are a powerful tool for the estimation of brine composition (Lowenstein et al., 2001, 2003; Horita et al., 2002; Brennan et al., 2004). A second technique, fluid inclusion microthermometry, is grounded on the fact that dissolved salts depress the freezing (and melting) temperature of water (ice). Few studies have used this technique on fluid inclusion in modern and ancient gypsum to determine brine salinities (e.g., Sabouraud-Rosset, 1976; Attia et al., 1995).

Here we present results from fluid inclusions in gypsum from the Messinian Primary Lower Gypsum unit (Roveri et al., 2008) of the Piedmont Basin (NW Italy) and from modern gypsum from the Conti Vecchi solar saltworks (Sardinia, Italy). We compare the melting behavior of fluid inclusions in modern marine gypsum, for which the composition and salinity of the parent brines are known, with that of the inclusions trapped in Messinian gypsum, for which the parent water chemistry is unknown. This comparative study reveals that Messinian gypsum did not form from the normal evaporation of seawater.

## THE MESSINIAN PRIMARY LOWER GYPSUM

The Primary Lower Gypsum (PLG; CIESM, 2008; Roveri et al., 2008) formed during the first stage of the Messininan salinity crisis (5.97–5.60 Ma; Manzi et al., 2013) in silled

peripheral basins of the Mediterranean area (Lugli et al., 2010; Fig. 1A). The marked lithologic cyclicity of these deposits, defined by decametric-scale gypsum-mud couplets, is ascribed to precession-driven dry-wet climate oscillations (Krijgsman et al., 1999).

We analyzed gypsum samples collected in two sections of the Piedmont Basin (Banengo and Moncucco; Dela Pierre et al., 2007; 2011; Natalicchio et al., 2013; Fig. 1B) showing the lowermost four PLG cycles made up of 15–30 m-thick gypsum beds, interbedded with 1–2 m-thick mudstone layers (Fig. 2A). The lowermost three gypsum beds consist of massive selenite with meter to centimeter-sized twinned crystals (Fig. 2B); the fourth bed is made up of banded selenite, composed of centimeter and millimeter thick crystal crusts separated by clay laminae. The textures and thicknesses of the sampled gypsum beds are remarkably similar to the PLG deposits of the other Mediterranean basins (Lugli et al., 2010; Fig. 1A). In particular, alternations of millimeter to centimeter thick turbid and limpid intervals are observed in the re-entrant angle of the twinned crystals (Fig. 2B). The turbid intervals contain clay-rich aggregates, marine (e.g., *Trigonium* sp.) and brackish (e.g., *Surirella* sp.) water diatoms (Bonci, personal commun.), and curved filaments ("spaghetti-like structures"; Panieri et al., 2010). Limpid intervals are mostly devoid of solid inclusions.

## THE MODERN GYPSUM

Modern gypsum was sampled at the Conti Vecchi solar saltworks, Sardinia, a complex of ~50 gypsum and halite crystallizer ponds through which Mediterranean seawater is pumped in order to concentrate brine by evaporation. Gypsum crystals, up to 9 cm tall, with elongate asymmetric habits and curved faces, were sampled in spring 2012 from decimeter-sized domes (Fig. 2C) growing on the bottom of shallow ponds, less than 1 m in depth. The chemical composition of a typical gypsum pond brine is shown in Table 1.

## MICROTHERMOMETRIC ANALYSIS

Seven samples from the Messinian sections and three samples from the modern saltworks were used for microthermometry (Attia et al., 1995; see details of methodology in GSA Data Repository).

Three types of aqueous inclusions are trapped within Messinian gypsum. The first type is marked by three- to six-sided geometrical shapes (Figs. 2D, E); groups of inclusions, 10–130 μm in size, are present within the re-entrant angle of the crystals and are aligned parallel to crystal growth surfaces. These are considered primary inclusions and were used for microthermometric studies. All these inclusions consist of a single-phase liquid, which, after stretching by freezing, (see methods in the GSA Data Repository), became two-phase (liquid + vapor) (Fig. 2E). The second type consists of prismatic to rounded elongated inclusions, up to 100 μm long; they are arranged along the 010 cleavage plane, with the major axis parallel to the 100 plane (Fig. 2F), and are thus interpreted as secondary (e.g., Attia et al., 1995). The third type consists of micron-sized inclusions aligned along fractures, thus secondary or pseudo-secondary in origin.

Primary inclusions in Messinian gypsum froze at −40 °C to −60 °C, with simultaneous shrinkage of the vapor bubble. During heating, first melting was observed between −38 °C and −35 °C (Table DR1). With further heating two solid phases were observed: one, more abundant, had low relief and a rounded habit (probably ice); the other had high relief (probably hydrohalite, $NaCl{\cdot}2H_2O$). The putative hydrohalite completely melted between −23 °C and −19 °C ($Tm_{Hhl}$) and at higher temperatures only rounded ice crystals remained within inclusions (Fig. 2E). The final melting temperature of ice ($Tm_{ice}$) for 90 fluid inclusions was between −4.9 °C and −0.1 °C with the majority between −1.5 °C and −0.1 °C (Fig. DR1).

In the Conti Vecchi gypsum, primary inclusions, up to 200 μm in size, show elongated and triangular shapes (Fig. 2G). Secondary micron-sized inclusions, mainly aligned

along fractures, are also present. Three types of primary inclusions are observed: 1) single phase (aqueous); 2) two phase (aqueous + vapor); 3) three phase (aqueous + vapor + halite); only 1 and 2 phase inclusions were selected for microthermometry. They froze at temperatures below –55 °C. During heating, a first re-organization occurred between –55 °C and –45 °C corresponding to the first melting of Mg-chloride hydrate, the main ultra low temperature hydrated salt in frozen seawater (Davis et al., 1990). Between –30 °C and –21 °C, two solid phases with different relief and habit were distinguished. One solid melted completely at ~–21 °C (±0.2 °C), close to the NaCl-$H_2O$ eutectic point. This melted solid is clearly ice, and not hydrohalite, because of its low relief. Moreover the remaining un-melted solid phase (Fig. 2H), when re-cooled, exhibited the hexagonal habit diagnostic of hydrohalite (Davis et al., 1990). The final melting temperature of hydrohalite was between –0.5 °C and 0 °C (±0.2 °C).

## MODERN VERSUS MESSINIAN WATERS: TWO DIFFERENT CHEMICAL SYSTEMS

The salinities of modern and Messinian fluid inclusions (see GSA Data Repository) are shown on $Na^+$ *vs* $Cl^-$ and $Ca^{2+}$ *vs* $SO_4^{2-}$ plots, along with the computer-simulated evaporation of seawater (Fig. 3). Salinities from modern gypsum fluid inclusions (26 weight % NaCl equivalent) fall along the gypsum precipitation segment. The obtained values (Figs. 3A, B) are somewhat higher than the salinities of the corresponding solar saltworks brines (Table 1) because (1) some water may have been lost from inclusions by evaporation, or (2) the gypsum (and inclusions) formed from a more concentrated brine than that shown in Table 1. Nevertheless, microthermometry of modern fluid inclusions predicts that the brines from which gypsum forms in marine settings are quite saline, from 11 to 27%.

Messinian fluid inclusions, in this study, have completely different chemical compositions; their salinities range from 0.2 to 7.7% (average 1.6 weight % NaCl

equivalent), indicating that the brine from which gypsum formed was depleted in $Na^+$ and $Cl^-$ relative to seawater (Figs. 3A, B). In comparison, gypsum first precipitates during the evaporation of modern seawater at a salinity of ~11%, corresponding to $Tm_{ice}$ of –7° to –8 °C (Attia et al., 1995). Remarkably, no Messinian fluid inclusions have salinities high enough to fall in the gypsum precipitation segment of the seawater evaporation curve (Fig. 3B). The only reasonable explanation of these results is that Messinian gypsum precipitated from brines with a significant proportion of non-marine waters.

## PALEOENVIRONMENTAL IMPLICATIONS

The non-marine composition of Piedmont Messinian fluid inclusions opens new questions concerning the $Ca^{2+}$ and $SO_4^{2-}$ sources necessary for the formation of thick gypsum deposits during the Messinian salinity crisis. The commonly accepted paleohydrologic models for the formation of the Primary Lower Gypsum (PLG) in the Mediterranean include evaporation of brines formed by continuous inflow of seawater from the Atlantic Ocean, providing the necessary ion supply, coupled with persistent reduced outflow during the precessional insolation minima (Krijgsman and Meijer, 2008; Topper and Meijer, 2013). A different mechanism, able to produce the lower salinity, $Ca^{2+}$ and $SO_4^{2-}$ enriched waters found in fluid inclusions in the PLG from the Piedmont Basin (PB), involves leaching ("recycling") of existing $CaSO_4$ evaporites by seawater, continental waters ("freshwater"), or a combination of the two (e.g., Cendón et al., 2004; Lowenstein and Risacher, 2009). Fluid inclusions composed of seawater or freshwater that have dissolved gypsum to reach saturation have final ice melting temperatures of –2° and ~0 °C, respectively (Attia et al., 1995). Those ice melting temperatures bracket the $Tm_{ice}$ of most of the studied samples (–1.5 °C < $Tm_{ice}$ <–0.2 °C), which suggests that the parent waters of the PLG were mixtures of seawater and continental waters that recycled pre-existing gypsum. Inflow of continental

freshwaters is required for all samples with fluid inclusion ice melting temperatures above –2 °C, the temperature of final ice melting for seawater with recycled $CaSO_4$.

Sulfur isotope values from Messinian sulfates in the PB ($\delta^{34}S$~22‰; Fontes et al., 1987) are diagnostic of Messinian seawater and/or recycled Messinian gypsum sources of sulfate; a few values ($\delta^{34}S$~10‰) may indicate precipitation from continental freshwater enriched in sulfate dissolved from Alpine Permian and Triassic evaporites (Fontes et al., 1987). Strontium isotope values from Piedmont gypsum ($0.70895 < {}^{87}Sr/{}^{86}Sr < 0.70899$; Bernardi, personal commun.) also suggest Messinian seawater or recycled Messinian gypsum Sr sources (Flecker et al., 2002; Lu and Meyers, 2003; Lugli et al., 2010). Sulfur and strontium isotopes confirm seawater inflow to the PB. Contemporaneous low salinity freshwater inflow contributed water to the PB but did little to influence the Messinian seawater signal demonstrated by S and Sr isotopes. Mixed seawater-freshwater inflow is also supported by the marine and freshwater diatoms found in the PLG.

The apparent paradox of Messinian gypsum formed from non-marine waters can be explained by considering short-term changes of the hydrological budget of marginal basins (Manzi et al., 2012). Deposition of the PLG deposits is here interpreted as follows: 1) during the dry season evaporative concentration caused the formation of brines and, eventually, the precipitation of gypsum. In the deepest anoxic settings saturation was not reached and no gypsum was deposited (de Lange and Krijgsman, 2010); 2) during the wet season, undersaturated continental waters (e.g., fluvial floods) partially or totally dissolved previously formed marine gypsum at the shallow water margins of the PB, producing waters enriched in $Ca^{2+}$ and $SO_4^{2-}$ but impoverished in $Na^+$ and $Cl^-$. Those “mixed” brines were the parent waters for gypsum precipitation by evaporative concentration during the transition to the next dry cycle.

This model for the PB needs to be tested for other Mediterranean PLG deposits, in order to solve the conundrum of similar evaporite facies deposited under different hydrological conditions. The PLG deposits show a surprisingly similar facies association and stacking pattern across the whole Mediterranean (Lugli et al., 2010), suggesting shared depositional conditions. On the other hand the stable isotope datasets (e.g., Pierre and Fontes, 1978) point to a system of sub-basins characterized by different marine and continental water inflows because of their paleogeographic position or local climate. Future studies will also focus on the gypsum organic content and the possible role of microbially-mediated redox reactions in sulfate enrichment and gypsum precipitation.

## CONCLUSIONS

The results of the first detailed analysis of fluid inclusion salinities in Messinian gypsum crystals provide new constraints for hydrologic models explaining widespread gypsum precipitation in marginal basins during the first stage of the Messinian salinity crisis. This study demonstrates that at the northernmost offshoot of the Mediterranean Basin, gypsum did not form just from pristine evaporated seawater but rather from a mix of seawater and $Ca^{2+}$ and $SO_4^{2-}$ enriched non-marine waters probably derived from partial dissolution and recycling of coeval marginal marine deposits. Complex recycling processes should also be taken in account for explaining the genesis of other similar Messinian gypsum deposits across the Mediterranean Basin.

## ACKNOWLEDGMENTS

Research funded by Compagnia di San Paolo (ProGEO Piemonte project) and University of Torino funds to F. Dela Pierre, MIUR grant to M. Roveri (PRIN 2008), NSF Geobiology and Low Temperature Geochemistry Award EAR-1024692 to T.K. Lowenstein. We thank B.C. Schreiber and P. Meijer for their constructive reviews, M.C. Bonci for diatoms determinations, Fassa Bortolo and Saint-Gobain for the permission to

sample their quarries and Saline Conti Vecchi for the water and gypsum sampling at their saltworks.

## REFERENCES CITED

Attia, O.E., Lowenstein, T.K., and Wali, A.M.A., 1995, Middle Miocene gypsum, Gulf of Suez: Marine or nonmarine?: Journal of Sedimentary Research, v. 65, p. 614–626.

Brennan, S.T., Lowenstein, T.K., and Horita, J., 2004, Seawater chemistry and the advent of biocalcification: Geology, v. 32, p. 473–476, doi:10.1130/G20251.1.

Cendón, D.I., Peryt, T.M., Ayora, C., Pueyo, J.J., and Taberner, C., 2004, The importance of recycling processes in the Middle Miocene Badenian evaporite basin (Carpathian foredeep): Palaeoenvironmental implications: Palaeogeography, Palaeoclimatology, Palaeoecology, v. 212, p. 141–158, doi:10.1016/j.palaeo.2004.05.021.

CIESM, 2008. The Messinian Salinity Crisis from mega-deposits to microbiology—A consensus report, *in* Briand, F., ed., CIESM Workshop Monographs 33, Monaco, 168 p.

Davis, D.W., Lowenstein, T.K., and Spencer, R.J., 1990, Melting behavior of fluid inclusions in laboratory-grown halite crystals in the systems NaCl-$H_2O$, NaCl-KCl-$H_2O$, NaCl-$MgCl_2$-$H_2O$, and NaCl-$CaCl_2$-$H_2O$: Geochimica et Cosmochimica Acta, v. 54, p. 591–601, doi:10.1016/0016-7037(90)90355-O.

de Lange, G.J., and Krijgsman, W., 2010, Messinian salinity crisis: A novel unifying shallow gypsum/deep dolomite formation mechanism: Marine Geology, v. 275, p. 273–277, doi:10.1016/j.margeo.2010.05.003.

Dela Pierre, F., Festa, A., and Irace, A., 2007, Interaction of tectonic, sedimentary, and diapiric processes in the origin of chaotic sediments: An example from the Messinian of Torino Hill (Tertiary Piedmont Basin, northwestern Italy): Geological Society of America Bulletin, v. 119, p. 1107–1119, doi:10.1130/B26072.1.

Dela Pierre, F., Bernardi, E., Cavagna, S., Clari, P., Gennari, R., Irace, A., Lozar, F., Lugli, S., Manzi, V., Natalicchio, M., Roveri, M., and Violanti, D., 2011, The record of the Messinian salinity crisis in the Tertiary Piedmont Basin (NW Italy): The Alba section revisited: Palaeogeography, Palaeoclimatology, Palaeoecology, v. 310, p. 238–255, doi:10.1016/j.palaeo.2011.07.017.

Flecker, R., De Villiers, S., and Ellam, R., 2002, Modelling the effect of evaporation on the salinity–87Sr/86Sr relationship in modern and ancient marginal-marine systems: the Mediterranean Messinian Salinity Crisis: Earth and Planetary Science Letters, v. 203, p. 221–233, doi:10.1016/S0012-821X(02)00848-8.

Fontes, J.C., Filly, A., and Gaudant, J., 1987, Conditions de depot du Messinien évaporitique des environs d'Alba (Piémont): Arguments paléontologiques et isotopiques: Bollettino della Società Paleontologica Italiana, v. 26, p. 199–210.

Horita, J., Zimmermann, H., and Holland, H.D., 2002, Chemical evolution of seawater during the Phanerozoic: Implications from the record of marine evaporites: Geochimica et Cosmochimica Acta, v. 66, p. 3733–3756, doi:10.1016/S0016-7037(01)00884-5.

Krijgsman, W., and Meijer, P., 2008, Depositional environments of the Mediterranean "Lower Evaporites" of the Messinian salinity crisis: Constraints from quantitative analyses: Marine Geology, v. 253, p. 73–81, doi:10.1016/j.margeo.2008.04.010.

Krijgsman, W., Hilgen, F.J., Raf, I., Sierro, F.J., and Wilson, D.S., 1999, Chronology, causes and progression of the Messinian salinity crisis: Nature, v. 400, p. 652–655, doi:10.1038/23231.

Longinelli, A., 1979, Isotope geochemistry of some Messinian evaporites; paleoenvironmental implications: Palaeogeography, Palaeoclimatology, Palaeoecology, v. 29, p. 95–123, doi:10.1016/0031-0182(79)90076-2.

Lowenstein, T.K., and Risacher, F., 2009, Closed basin brine evolution and the influence of Ca–Cl inflow waters: Death Valley and Bristol Dry Lake California, Qaidam Basin, China, and Salar de Atacama, Chile: Aquatic Geochemistry, v. 15, p. 71–94, doi:10.1007/s10498-008-9046-z.

Lowenstein, T.K., Timofeeff, M.N., Brennan, S.T., Hardie, L.A., and Demicco, R.V, 2001, Oscillations in Phanerozoic seawater chemistry: evidence from fluid inclusions: Science, v. 294, 5544, p. 1086–1088, doi:10.1126/science.1064280.

Lowenstein, T.K., Hardie, L.A., Timofeeff, M.N., and Demicco, R.V., 2003, Secular variation in seawater chemistry and the origin of calcium chloride basinal brines: Geology, v. 31, p. 857, doi:10.1130/G19728R.1.

Lu, F.H., and Meyers, W.J., 2003, Sr, S, and $O_{SO4}$ isotopes and the depositional environments of the upper Miocene evaporites, Spain: Journal of Sedimentary Research, v. 73, p. 444–450, doi:10.1306/093002730444.

Lugli, S., Manzi, V., Roveri, M., and Schreiber, B.C., 2010, The Primary Lower Gypsum in the Mediterranean: A new facies interpretation for the first stage of the Messinian salinity crisis: Palaeogeography, Palaeoclimatology, Palaeoecology, v. 297, p. 83–99, doi:10.1016/j.palaeo.2010.07.017.

Manzi, V., Gennari, R., Lugli, S., Roveri, M., Scafetta, N., and Schreiber, B.C., 2012, High-frequency cyclicity in the Mediterranean Messinian evaporites: Evidence for solar-lunar climate forcing: Journal of Sedimentary Research, v. 82, p. 991–1005, doi:10.2110/jsr.2012.81.

Manzi, V., Gennari, R., Hilgen, F., Krijgsman, W., Lugli, S., Roveri, M., and Sierro, F.J., 2013, Age refinement of the Messinian salinity crisis onset in the Mediterranean: Terra Nova, v. 25, p. 315–322, doi:10.1111/ter.12038.

Natalicchio, M., Dela Pierre, F., Clari, P., Birgel, D., Cavagna, S., Martire, L., and Peckmann, J., 2013, Hydrocarbon seepage during the Messinian salinity crisis in the Tertiary Piedmont Basin (NW Italy): Palaeogeography, Palaeoclimatology, Palaeoecology, v. 390, p. 68–80, doi:10.1016/j.palaeo.2012.11.015.

Panieri, G., Lugli, S., Manzi, V., Roveri, M., Schreiber, B.C., and Palinska, K.A, 2010, Ribosomal RNA gene fragments from fossilized cyanobacteria identified in primary gypsum from the late Miocene, Italy: Geobiology, v. 8, p. 101–111, doi:10.1111/j.1472-4669.2009.00230.x.

Pierre, C., and Fontes, J.C., 1978, Isotope composition of Messinian sediments from the Mediterranean Sea as indicators of paleoenvironments and diagenesis, *in*: Hsü, K.J., and Montadert, L., eds Initial Reports of the Deep Sea Drilling Project, Leg XLIIA, Washington, US Government Printing Office, v. 42A, p. 635–650.

Roveri, M., Lugli, S., Manzi, V., and Schreiber, B.C., 2008, The Messinian Sicilian stratigraphy revisited: new insights for the Messinian Salinity Crisis: Terra Nova, v. 20, p. 483–488.

Sabouraud-Rosset, C., 1976, Solid and liquid inclusions in gypsum [unpublished These d'Etat]: Paris, Université Paris Sud, Centre d'Orsay, 173 p.

Topper, R.P.M., and Meijer, P.T., 2013, A modeling perspective on spatial and temporal variations in Messinian evaporite deposits: Marine Geology, v. 336, p. 44–60, doi:10.1016/j.margeo.2012.11.009.

**FIGURE CAPTIONS**

Figure 1. A: Distribution of the Messinian evaporites (gypsum and halite) in the Mediterranean Basin (after Lugli et al., 2010 and Manzi et al., 2012). PB: Piedmont Basin; CV: Conti Vecchi saltworks. B: Geological sketch of the studied area showing the

distribution of the Messinian sulfates and of the sampled sections (M: Moncucco; B: Banengo).

Figure 2. Messinian and modern gypsum. A: Panoramic view of the Moncucco quarry: three Primary Lower Gypsum couplets, composed of mud (M; dashed lines) and gypsum (G), are visible; arrows indicates the gypsum growth direction. B: Twinned Messinian selenite crystal; TI: turbid interval; LI: limpid interval. C: Modern gypsum dome, Conti Vecchi saltworks; arrows point to dissolution surfaces among cm-sized crystal palisades. D,E,F: Photomicrographs of primary (D, E) and secondary (F) fluid inclusions in Messinian crystals (transmitted light); E shows a primary fluid inclusion near the $Tm_{ice}$, with ice, liquid, and vapor. G,H: Photomicrographs of primary fluid inclusions in modern gypsum (transmitted light); H shows melting of hydrohalite microcrystals in the presence of liquid and vapor.

Figure 3. $Na^+$ *vs* $Cl^-$ (A) and $Ca^{2+}$ *vs* $SO_4^{2-}$ (B) diagrams showing the curve tracking computer simulation of the evaporation of modern seawater (see details in GSA Data Repository) and the composition of the Conti Vecchi brine (circle). Messinian (bars) and modern (vertical dashed line) fluid inclusions salinities are reported as weight % NaCl equivalent (bottom scale). Vertical axis on the left refers to the number of Messinian fluid inclusions. The salinity of modern seawater is also reported for comparison (vertical line). The minerals predicted to precipitate during progressive evaporation of seawater are shown as horizontal bars at the bottom.

[1]GSA Data Repository item 2014XXX sampling, methodology and Messinian fluid inclusion data (Table DR1, Figure DR1) are available online at www.geosociety.org/pubs/ft2014.htm, or on request from editing@geosociety.org or Documents Secretary, GSA, P.O. Box 9140, Boulder, CO 80301, USA.

TABLE 1. CONTI VECCHI BRINE COMPOSITION

| Sample name | Cl (*) | $SO_4$ (*) | Br (*) | Ca (*) | K (*) | Mg (*) | Na (*) | Sr (*) | Conductivity (mS/cm) | Salinity (PSU) | Density (g/mL) |
|---|---|---|---|---|---|---|---|---|---|---|---|
| CV1 | 4070 | 158 | 5.8 | 25 | 105 | 522 | 3980 | 0.5 | 211 | 212 | 1.15 |

*Note:* (*) Units are in millimols solute per kg $H_2O$

Publisher: GSA
Journal: GEOL: Geology
Article ID: G34986

316 FIGURES

317

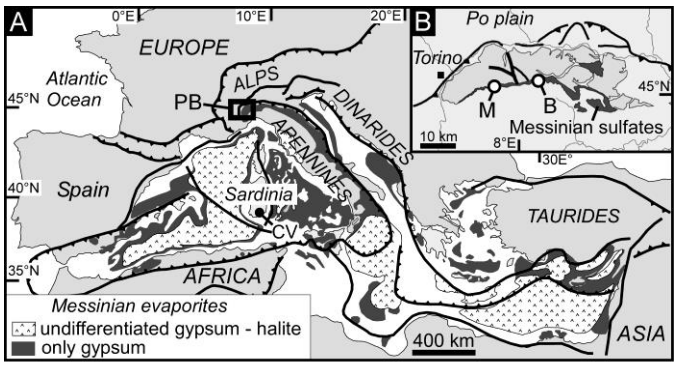


318 Natalicchio et al. Fig. 1 (JPG)

319

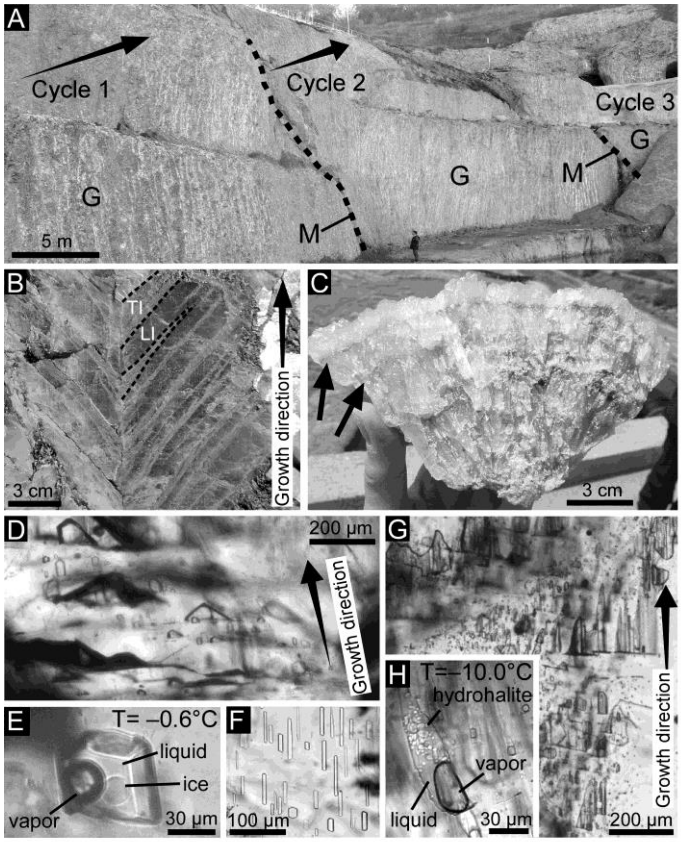


320 Natalicchio et al. Fig. 2 (JPG)

321

Publisher: GSA
Journal: GEOL: Geology
Article ID: G34986

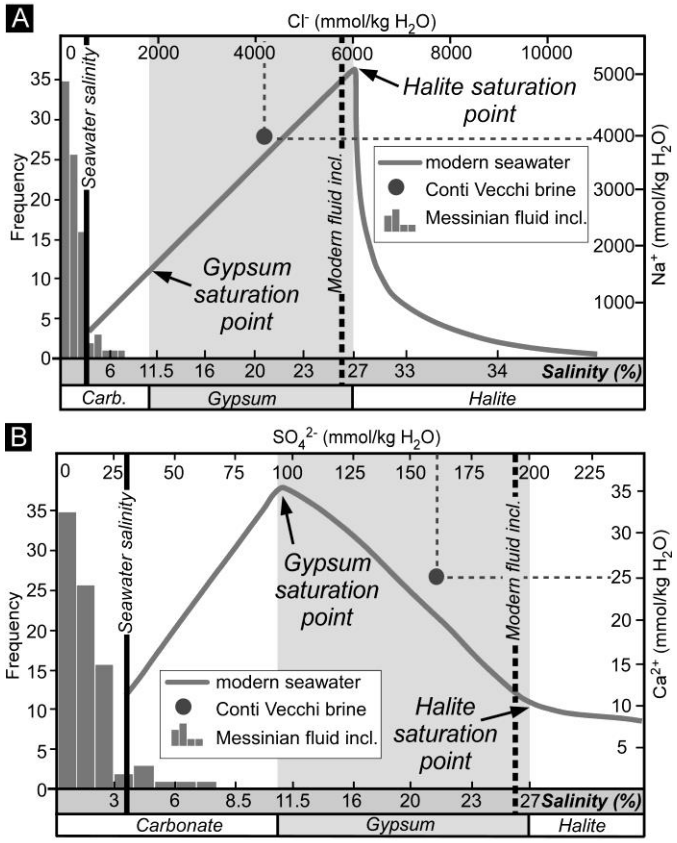


322 Natalicchio et al. Fig. 3 (JPG)

323